宇野賀津子（ルイ・パストゥール医学研究センター）

4) 関節リウマチの治療：橋本博史（順天堂大・膠原病内科）

5) 非対称性脳萎縮が先行し，ガンマグロブリン療法が奏効したSLEの1例：
山西裕司（広島市民病院リウマチ科）

6) 急性期川崎病においてIVIGによるoxydant stressの抑制作用：
高月晋一、竹内大二、佐地　勉（東邦大・医・第一小児科）

7) RPGNの治療：有村義宏（杏林大・医）

8) 家庭血圧計およびデータ自動転送システムを用いた高血圧治療介入試験：
山崎力（東京大・院医・クリニカルバイオインフォマティクス研究ユニット）

4．基礎班と臨床班の総合討論

5．事務連絡

研究成果の刊行に関する一覧表

雑誌

発表者氏名	論文タイトル名	発表誌名	巻号	ページ	出版年
T. Oharaseki, Y. Kameoka, F. Kura, A.S. Persad, **K. Suzuki**, S. Naoe.	Susceptibility loci to coronary arteritis in animal model of Kawasaki disease induced with *Candida albicans*-derived substances.	Microbiol Immunol.	49	181-189	2005
A. Hoshino, K. Fujioka, T. Oku, S. Nakayama, M. Suga, Y. Yamaguchi, **K. Suzuki**, K., M. Yasuhara, K. Yamamoto	Quantum dots targeted to the assigned organelle in living cells	Microbiol. Immnol.	48	985-994	2004
A. Hoshino, K. Fujioka, T. Oku, M. Suga, Y.F. Sasaki, T. Ohta, M. Yasuhara, **K. Suzuki**, and K. Yamamoto.	Physicochemical Properties and Cellular Toxicity of Nanocrystal Quantum Dots Depend on Their Surface Modification	Nanolett	4	2163-2169	2004
N. Nagai-Miura, Y. Shingo, Y. Adachi, A. Ishida-Okawara, T. Oharaseki, K. Takahashi, S. Naoe, **K. Suzuki** and N. Ohno.	Induction of Coronary Arteritis with Administration of CAWS (*Candida albicans* Water-Soluble Fraction) Depending on Mouse Strains.	Immunopharmacol. Immunotoxicol.	26	527-543	2004
K. Suzuki, E. Muso and W. Nauseef.	Contribution of Peroxidases in Host-defense, Diseases and Cellular Functions.	Jpn. J. Infect. Dis.	57	S1-2	2004
K. Suzuki and T. Okazaki.	Contribution of myeloperoxidase in vasculitis development	Jpn. J. Infect. Dis.	57	S2-3	2004
Y. Kameoka, A. S. Persad and **K. Suzuki**.	Genomic variations in myeloperoxidase gene in the Japanese population.	Jpn. J. Infect. Dis.	57	S12-13	2004
Y. Aratani, F. Kura, H. Watanabe, H. Akagawa, Y. Takano, **K. Suzuki**, M.C. Dinauer, N. Maeda, and H. Koyama.	In vivo role of myleloperoxidase for the host defense.	Jpn. J. Infect. Dis	57	S15	2004
E. Muso, T. Ito-Ihara, T. Ono, E. Imai, K. Yamagata, A. Akamatsu, **K. Suzuki**.	Intravenous immunoglobulin (IVIg) therapy in MPO-ANCA related polyangiitis with rapidly progressive glomerulonephritis in Japan	Jpn. J. Infect. Dis	57	S17-18	2004
Shiohara A, Hoshino A, Hanaki K, **Suzuki K**, and Yamamoto K.	On the cyto-toxicity caused by quantum dots.	Microbiol Immunol.	48	669-676	2004.
Ito, M., Nagata, N., Yumoto, F., Yamagoe, S., **Suzuki, K.**, Adachi, K. and Tanokura, M.	^{1}H, ^{13}C, ^{15}N resonance assignments of the cytokine LECT2.	Journal of Biomolecular NMR	29	543-544	2004.
C. Ovejero, C. Cavard, A. Perianin, T. Hakvoort, J. Vermeulen, C. Godard, M. Fabre, P. Chafey, **K. Suzuki**, B. Romagnolo, S. Yamagoe, C. Perret..	Identification of the leukocyte cell-derived chemotaxin2 (LECT2) as a direct target gene of s-catenin in the liver	Hepatology	40	167-176	2004
T. Saito, A. Okumura, H. Watanabe, M. Asano, A. Ishida-Okawara, J. Sakagami, K. Sudo, Y.	Increase of Hepatic NKT Cells in LECT2-Deficient Mice Contributes to Severe Concanavalin A-Induced Hepatitis.	J Immunol	173	579-585	2004.

Hatano-Yokoe, T. Abo, Y. Iwakura, **K. Suzuki**, and S. Yamagoe.					
S. Suzuki, K. Honma, T. Matsuyama, **K. Suzuki**, K. Toriyama, K. Yamamoto, K. Miyazaki, M. Nakamura, K. Yu, A. Kumatori.	Critical roles of Interferon regulatory factor-4 in $CD11b^{high}CD8^{-}$ dendritic cell development	Proc Natl Acad Sci USA.	101	8981-8986	2004
A. Ishida-Okawara, T. Ito-Ihara, E. Muso, T. Ono, K. Saiga, K. Nemoto, **K. Suzuki**.	Neutrophil contribution to the crescentic glomerulonephritis in SCG/Kj mice.	Nephrol., Dial. Transplant	19	1708-1715	2004
Ohashi, Y.Y., Kameoka, Y., Persad, A.S., Kohi, F., Yamagoe, S., Hashimoto, K., and **Suzuki, K.**.	Novel missense mutation found in Japanese patient with myeloperoxidase deficiency.	Gene	327	195-200	2004
Hoshino, A., Hanaki, K., **Suzuki, K.** and Yamamoto, K.,	Applications of T-lymphoma labeled with fluorescent quantum dots to cell tracing markers in mouse body	Biochem. Biophys. Res. Comm.	314	46–53	2004
鈴木和男	バイオイメージングが切り開く新たな診断・治療評価技術	医学のあゆみ	210	171	2004
長尾朋和、鈴木和男	血管炎初期反応のイメージング	医学のあゆみ	210	196-199	2004
長尾朋和、村山 研、越尾 修、大野尚仁、三浦典子、高橋 啓、馬渕綾子、南谷晴之、鈴木和男	腎臓血管傷害のイメージング	PharmaMedica	22	185-189	2004
武曾恵理、猪原登志子	血管炎症候群と免疫グロブリン大量療法	リウマチ科	31(1)	67-74	2004
米本智美、田中麻理、南方保、武曾恵理	他臓器（胃）で発見され、腎生検にて確認されたANCA関連血管炎の１例	Pharma Medica	22(5)	182-184	2004
糟野健司、武曾恵理、小野孝彦、中村肇、淀井芳子、淀井省三、糟野裕子、児玉直也、東義人、大伴裕美子、淀井淳司	透析患者における酸化ストレスマーカー、チオレドキシン(TRX)と脂質について	*Therapeutic Res*	25.9	1802-1804	2004
武曾恵理、 糟野健司	腎虚血再灌流とレドックス	医学のあゆみ	印刷中		
宇野賀津子、古宮俊幸、猪原登志子、田原佐知子、田中麻理、米本智美、塚本達雄、深津敦司、北 徹, 岸田綱太郎、鈴木和男、武曾恵理	MPO-ANCA 関連急速進行性腎炎再発症例におけるガンマグロブリン大量投与療法（IVIg）前後の免疫動態	PasKen J	印刷中		2004
武曾恵理、猪原登志子、宇野賀津子	難治性腎疾患治療の新たな展開—ANCA 関連腎炎の大量グロブリン療法	先端医療シリーズ３１「腎臓病—診断と治療の最前線」	印刷中		
Ono T, Liu N, Makino T, Nogaki F, Nomura K, Muso E, Shimizu F, Honda G, Kita T.	Role of Mesangial Factor V Expression in the Crescent Formation in Rat Experimental Mesangioproliferative Glomerulonephritis	*J Pathol*	204(2)	229-38	2004

Oida E, Nogaki F, Kobayashi I, Kamata K, Ono T, Miyawaki S, Serikawa T, Yoshida Y, Kita T and Muso E.	Quantitative trait loci (QTL) analysis reveals a close linkage between the hinge region and trimeric IgA dominancy in a high IgA strain (HIGA) of ddY mice	*Eur J Immunol*	34(8)	2200-8	2004
Hirashima M, Fukazawa T, Abe K, Morita Y, Kusaoi M, Hashimoto H.	Expression and activity analysis of CTLA4 in peripheral blood lymphocytes in systemic lupus erythematosus	Lupus	13	24-31	2004
Matsuda Y, Tsuda H, Takasaki Y, Hashimoto H.	Double filtration plasmapheresis for the treatment of a rheumatoid arthritis patient with extremely high level of C-reactive protein	Ther Apher Dial	8	404-408	2004
Kempe K, Tsuda H, Yang K, Yamaji K, Kanai Y, Hashimoto H.	Filtration leukocytapheresis therapy in the treatment of rheumatoid arthritis patients resistant to or failed with methotrexate	Ther Apher Dial	8	197-205	2004
Chiba A, Oki S, Miyamoto K, Hashimoto H, Yamamura T, Miyake S.	Suppression of collagen-induced arthritis by natural killer T cell activation with OCH, a sphingosine-truncated analog of alpha-galactosylceramide	Arthritis Rheum	50	305-313	2004
Liu H, Hanawa H, Yoshida T, Elnaggar R, Hayashi M, MD RW, Toba K, Yoshida K, Chang H, Okura Y, Kato K, Kodama M, Maruyama H, Miyazaki J, Nakazawa M, **Aizawa Y.**	Effect of Hydrodynamics-Based Gene Delivery of Plasmid DNA Encoding IL-1 Receptor Antagonist-Ig for Treatment of Rat Autoimmune Myocarditis: Possible Mechanism for Lymphocytes and Non-Cardiac Cells.	Circulation.	In press		
Abe Y, Watanabe K, Sato S, Nagai Y, Kamal FA, Wahed MI, Wen J, Narasimman G, Ma M, Suresh P, Takahashi T, Tachikawa H, Kashimura T, Tanabe N, Kodama M, **Aizawa Y**, Yamaguchi K, Miyazaki M, Kakemi M.	Hemodynamic effects of carvedilol infusion and the contribution of the sympathetic nervous system in rats with heart failure	Pharmacology. Dec	72(4)	213-9	2004
Abe S, Okura Y, Hoyano M, Kazama R, Watanabe S, Ozawa T, Saigawa T, Hayashi M, Yoshida T, Tachikawa H, Kashimura T, Suzuki K, Nagahashi M, Watanabe J, Shimada K, Hasegawa G, Kato K, Hanawa H, Kodama M, **Aizawa Y.**	Plasma concentrations of cytokines and neurohumoral factors in a case of fulminant myocarditis successfully treated with intravenous immunoglobulin and percutaneous cardiopulmonary support.	Circ J	68	1223-6	2004
Kodama M,Kato K,Hirono S,Okura Y,Hanawa H,Yoshida T, Hayashi M,Tachikawa H,Kashimura T,Watanabe K, **Aizawa Y.**	Linkage Between Mechanical and Electrical Alternans in Patients with Chronic Heart Failure	Journal of Cardiovascular Electrophysiology	15	295-299	2004
Hanawa H,Watanabe R,Hayashi M, Yoshida T, Abe S,Komura S,	A Novel Method to Assay Proteins in Blood Plasma after Intravenous Injection of	J.Exp.Med	202	155-161	2004

Lui H,,Elnaggar R,Chang H,Okura Y,Kato K,Kodama M,Maruyama H,Miyazaki J,**Aizawa Y.**	Plasmid DNA. Tohoku				
Kashimura T, Kodama M, Hotta Y, Hosoya J, Yoshida K, Ozawa T, Watanabe R, Okura Y, Kato K, Hnawa H, Kuwano R, **Aizawa Y.**	Spatiotemporal changes of coxsackievirus and adenovirus receptor in rats hearts during postnatal development and in cultured cardiomyocytes of neonatal rat	Vichows Arch	444	283-292	2004
Nasuno A, Toba K, Ozawa T, Hanawa H, Osman Y, Hotta Y, Yoshida K, Saigawa T, Kato K,Kuwano R, Watanabe K, **Aizawa Y.**	Expression of coxsackievirus and adenovirus receptor in neointima of the rat carotid artery. Cardiovascular	Pathology	13	79-84	2004
Wahed MI, Watanabe K, Ma M, Yamaguchi K, Takahashi T, Tachikawa H, Kodama M, **Aizawa Y.**	Effects of Eplerenone, a Selective Aldosterone Blocker, on the Progression of Left Ventricular Dysfunction and Remodeling in Rats with Dilated Cardiomyopathy	Pharmacology	73(2)	81-88	2004
Wahed MI, Watanabe K, Ma M, Nakazawa M, Takahashi T, Hasegawa G, Naito M, Yamamoto T, Kodama M, **Aizawa Y.**	Effects of pranidipine, a novel calcium channel antagonist, on the progression of left ventricular dysfunction and remodeling in rats with heart failure	Pharmacology	72(1)	26-32	2004
佐地 勉, 薗部友良, 上村 茂, 赤木禎治, 鮎澤 衛	川崎病急性期治療のガイドライン	日小循誌	20, 1	54-62	2004
Onouchi Y, Onoue S, Tamari M, et al,	(19th place): CD40 ligand gene and Kawasaki disease. Eur J of Human	Gene	12	1062-1068	2004
佐地 勉, (ゲスト)川崎富作	川崎病と闘う日々ー川崎富作先生に聞く Part1.心臓		37	161-168	2005
Naohito Ohno	Murine Model of Kawasaki Disease Induced by Mannoprotein-β-Glucan Complex, CAWS, Obtained from *Candida albicans*	*Jpn. J. Infect. Dis*	57	9-10	2004
Ken-ichi Ishibashi, Noriko N. Miura, Yoshiyuki Adachi, Norihiko Ogura, Hiroshi Tamura, Shigenori Tanaka, and Naohito Ohno	DNA Array Analysis of Altered Gene Expression in Human Leukocytes Stimulated with Soluble and Particulate Forms of *Candida* Cell Wall β-Glucan	*Int. Immunopharmacol*	4	387-401	2004
Toshie Harada, Noriko N. Miura, Yoshiyuki Adachi, Mitsuhiro Nakajima, Toshiro Yadomae, and Naohito Ohno	Granulocyte-Macrophage Colony-Stimulating Factor (GM-CSF) Regulates Cytokine Induction by 1,3-β-D-Glucan SCG in DBA/2 Mice In Vitro	*J. Interferon Cytokine Res*	24	478-489	2004
Maruyama, K., Ohuchi, T., Yoshida, K., Shibata, Y., Sugawara F. and Arai, T.	Protective properties of neoechinulin A against SIN-1-induced neuronal cell death	J. Biochem.	136	81-87	2004
新井孝夫	モノクローナル抗体をもちいたポリグルタミン酸化チューブリンの神経細胞内局在	実験医学	22	1876-1877	2004

Okada, Y., Suzuki, A., Takagi' S., Hirai, H., Saitoh' R., Adachi, A., Yanagisawa, T., Ueki' M., Fujii' T. and Arai, T.	Polyglutamylation of tubulin during differentiation of neural precursor cells	Bioimages	in press		
K.Takahashi,T. Oharaseki, M.Wakayama,Y.Yokou chi, S. Naoe and H. Murata	Histopathological features of murine systemic vasculitis caused by *Candida albicans* extract – an animal model of Kawasaki Disease	Inflamm. res	53	72–77	2004
Sugo, N., Niimi, N., Aratani, Y., Takiguchi-Hahashi, K., and Koyama, H	p53 deficiency rescues neuronal apoptosis but not differentiation in DNA polymerase □-deficient mice	Mol. Cell Biol	24	9470-9477	2004

Microbiol. Immunol., 49(2), 181–189, 2005

Editor-Communicated Paper

Susceptibility Loci to Coronary Arteritis in Animal Model of Kawasaki Disease Induced with *Candida albicans*-Derived Substances

Toshiaki Oharaseki*[,1], Yosuke Kameoka[2], Fumiaki Kura[3], Amanda S. Persad[4], Kazuo Suzuki[4], and Shiro Naoe[1]

[1]*Department of Pathology, Ohashi Hospital, Toho University School of Medicine, Meguro-ku, Tokyo 153–8515, Japan,* [2]*Division of Genetic Resources,* [3]*Department of Bacteriology, and* [4]*Department of Bioactive Molecules, National Institute of Infectious Diseases, Shinjuku-ku, Tokyo 162–8640, Japan*

Communicated by Dr. Hidechika Okada: Received November 26, 2004. Accepted December 13, 2004

Abstract: **We have established an animal model of coronary arteritis which is histopathologically similar to that observed in cases of Kawasaki disease (KD), is a well-known childhood vasculitis syndrome. Coronary arteritis in this mouse model has been induced by intraperitoneal injection of *Candida albicans*-derived substances (CADS). Arteritis varied by mouse strain with the highest incidence by 71.1% (27/38) found in C3H/HeN mice, but absent in CBA/JN mice (0%, 0/27), suggesting association of genomic background to develop the disease. The present study aims to elucidate the susceptibility loci associated with coronary arteritis by using this animal model. The association of the onset of arteritis with polymorphic microsatellite markers between the two strains was examined using one hundred and fifteen of N1 backcross progeny [(CBA×C3H)F1×C3H]. Based on our analysis, arteritis-susceptibility loci with suggestive linkage were mapped on *D1Mit171* and *D1Mit245* (map position 20.2 cM) on chromosome 1 (P=0.0019). These loci include several kinds of inflammatory cytokine receptors, such as interleukin 1 receptor and tumor necrosis factor receptor. We also found the cytokine response against CADS, levels of inflammatory cytokines interleukin-1β, tumor necrosis factor-α, and interleukin-6 in sera increased within 24 hr after CADS injection. Our results may indicate based on genomics that ligand-receptor interaction between these inflammatory cytokines and the receptors of these cytokines may affect the onset of arteritis.**

Key words: **Kawasaki disease, Arteritis, *Candida albicans*, Interleukin 1 receptor, Chromosome mapping**

Kawasaki disease (KD) is an acute febrile mucocutaneous syndrome with systemic vasculitis mainly affecting infants and small children. The principal symptoms of KD are fever, congestion of ocular conjunctivae, reddening of lips and oral mucosa, swelling and reddening of palms and soles followed by peeling of skin, swelling of cervical lymph nodes coincidentally with systemic vasculitis (9). Inflammation of medium-sized muscular arteries, especially the coronary artery, is commonly associated with this disease. Ischemic heart disease with thrombotic occlusion, originating from coronary arteritis is a severe complication of KD. Histopathologically, it was reported that arteritis defined as 'productive granulomatous inflammation' was typical in KD cases (15, 19). This type of inflammation consists of dense infiltration of both neutrophils and histiocytes accompanied with a few lymphocytes. Mechanisms of developing arteritis in the patients with KD

**Address correspondence to* Dr. Toshiaki Oharaseki, Department of Pathology, Ohashi Hospital, Toho University School of Medicine, 2–17–6 Ohashi, Meguro-ku, Tokyo 153–8515, Japan. Fax: +81–3–3468–1283. E-mail: oharasek@muc.biglobe.ne.jp

Abbreviations: CADS, *Candida albicans* derived substances; cM, centi-morgan; ELISA, enzyme-linked immunosorbent assay; EvG, Elastica van Gieson; HE, hematoxylin and eosin; IFN-γ, interferon-γ; IL, interleukin; *Il1r1*, interleukin-1 receptor type 1; *Il1r2*, interleukin-1 receptor type 2; KD, Kawasaki disease; MCLS-6, mucocutaneous lymphnode syndrome-6; MPO, myeloperoxidase; MPO-ANCA, myeloperoxidase-antineutrophilic cytoplasmic antibody; PCR, polymerase chain reaction; QTL, quantitative trait of loci; TNF-α, tumor necrosis factor α; *Tnfrsf1b*, TNF receptor superfamily member 1b; *Tnfrsf8*, TNF receptor superfamily member 8; *Tnfrsf9*, TNF receptor superfamily member 9.

remain to be determined; however, there are some reports that coronary arteritis is affected by genetic polymorphism of several kinds of inflammatory cytokines, such as tumor necrosis factor α (TNF-α) (8), and interleukin-6 (IL-6) (7). Appropriate animal models of KD will allow for the clarification of the mechanisms governing the development of arteritis, and possibly, specific treatments for this disease. One of the animal models of arteritis that exist is the MRL/lpr mouse model. It is the standard animal model for studying systemic lupus erythematosus, with a common affliction to spontaneous arteritis. In MRL/lpr mice, some genes associated with arteritis have been elucidated (5). Recently, it was reported that arteritis in different tissues were under the control of different susceptibility loci (21).

Some infectious microorganisms, such as *Staphylococcus aureus* (11), *Streptococcus sanguis* (16), *Streptococcus pyogenes* (22), and *Rickettsia* (6) have been considered likely etiology candidates for this disease, though the primary causes remain unclear. These microorganisms are considered to act as the initial trigger for the development of arteritis in the patients with KD. Therefore, the initial trigger by an infectious microorganism is necessary for ideal model of KD to induce arteritis. However, this spontaneous arteritis model may not be well suited as an animal model for KD. On the other hand, Murata (13) has established a unique arteritis model that has been evaluated as an animal model of KD. In this model, arteritis induction is ascertained by injecting mice with alkaline extract of *Candida albicans* as an experimental arteritis. It should be noted that the quantity of this yeast was observed to be in elevated in stool samples of KD patients (14). The histology of this experimental arteritis model is similar to that of an autopsy case of KD (2). In this model, genetics in mice may have an influence on the development of arteritis. It was shown that the incidence of coronary arteritis varied by mouse strain, with the C3H/HeN mice having the highest incidence and coronary arteritis being absent in CBA/JN strains (20).

To identify susceptibility loci to the coronary arteritis, we analyzed coronary arteritis in [(CBA/JN×C3H/HeN)×C3H/HeN]N1 backcross progeny. The evidence presented herein shows that the susceptibility loci are linked to genes of several inflammatory cytokine receptors found in the coronary artery.

Materials and Methods

Chemicals. Sabouraud-2% dextrose broth (MERCK, Darmstadt, Germany) was used as culture medium. Sodium chloride, potassium hydroxide, acetic acid, ethanol, acetone, diethyl ether (Wako Pure Chemical Industries, Ltd., Osaka, Japan) and *n*-octyl alcohol (Kanto Chemical Co., Tokyo) were used for polysaccharide extraction from the cell wall of *C. albicans*.

Genomic DNA was isolated from whole blood obtained from the tail of animals using the QIAamp DNA mini kit (Qiagen, Hilden, Germany). FAM labeled primers for microsatellite markers were purchased from SIGMA Genosys Japan (Ishikari, Japan). Amplification and labeling of each microsatellite locus were performed by using Z-*Taq* polymerase (TaKaRa, Kyoto, Japan).

Animals. Mice, CBA/JNCrj (CBA/JN) and C3H/HeNCrj (C3H/HeN), were purchased from Charles River Japan (Astugi, Japan). Using C3H/HeN and CBA/JN strains, (C3H/HeN female×CBA/JN male)F1, (CBA/JN female×C3H/HeN male)F1, and [(CBA/JN×C3H/HeN)F1×C3H/HeN]N1 were prepared. N1 backcross progeny, 4-week-old males, were used for the linkage analysis (n=115). These mice were housed in a specific pathogen-free animal quarter and cared for under strict ethical guidelines.

Preparation of alkaline extract of C. albicans *(CADS).* CADS were prepared as follows. *C. albicans* (strain MCLS-6) isolated from the feces of patients with typical Kawasaki disease, was cultured in Sabouraud's dextrose medium with 2% glucose at 37 C. After a 72-hr incubation period, the yeast was harvested by centrifugation and extracted sequentially with boiling water, 0.1 M, and 0.5 M potassium hydroxide. After neutralization with acetic acid and dialysis against distilled water for 3 days, the extract was precipitated with ethanol. Four milligrams of the CADS, suspended in 0.2 ml of phosphate-buffered saline without calcium and magnesium (PBS(−)), were prepared as the inoculants.

Experimental schedule. Inoculation was conducted as described in the previous procedures (13). Namely, mice were injected once daily with 0.2 ml of inoculate intraperitoneally for 5 consecutive days during the first and fifth week. Each mouse was sacrificed with carbon dioxide asphyxiation at the ninth week and autopsied.

Histopathological evaluation of arteritis. The following visceral organs were obtained for histopathological examination: heart, aorta, kidney, lung, liver, pancreas, spleen, thymus, testis, muscle of hind leg, and spine. These specimens were fixed in 10% formalin and embedded in paraffin. Hematoxylin and eosin (HE) and Elastica van Gieson (EvG) stains were performed by routine histological techniques. Arteritis in individual mice was determined using light microscopy. A mouse with inflammation involving all layers of coronary artery and/or the aortic root was considered positive for coronary arteritis and used for linkage analysis.

Microsatellite markers. Two hundred and fifty-six markers (Fig. 1) were used for the linkage analysis between C3H/HeN and CBA/JN mice. Amplification and labeling of specific microsatellite loci were performed by using the polymerase chain reaction (PCR) with FAM labeled primers. Amplified DNA was analyzed with automated fragment analyzer ABI3700 and genotyped by Genescan software (Applied Biosystems, Japan).

Linkage analysis. Genotype distribution was compared among affected and non-affected N1 mice. Since the trait distribution was similar, we performed non-

Chromosome 1 (53)									
	D1Mcg101	D1Mcg2	D1Mcg3	D1Mcg4	D1Mcg6	D1Mit120	D1Mit121	D1Mit160	D1Mit160
	D1Mit161	D1Mit167	D1Mit17	D1Mit171	D1Mit180	D1Mit19	D1Mit200	D1Mit211	D1Mit230
	D1Mit24	D1Mit242	D1Mit245	D1Mit251	D1Mit298	D1Mit3	D1Mit303	D1Mit316	D1Mit318
	D1Mit321	D1Mit322	D1Mit363	D1Mit372	D1Mit373	D1Mit374	D1Mit380	D1Mit410	D1Mit427
	D1Mit429	D1Mit430	D1Mit431	D1Mit432	D1Mit465	D1Mit518	D1Mit52	D1Mit52.2	D1Mit520
	D1Mit58	D1Mit64	D1Mit66	D1Mit67	D1Mit7	D1Mit70	D1Mit73	D1Mit75	
Chromosome 2 (25)									
	D2Mit106	D2Mit110	D2Mit139	D2Mit166	D2Mit169	D2Mit194	D2Mit200	D2Mit206	D2Mit226
	D2Mit255	D2Mit258	D2Mit265	D2Mit304	D2Mit305	D2Mit307	D2Mit311	D2Mit413	D2Mit443
	D2Mit456	D2Mit457	D2Mit496	D2Mit51	D2Mit6	D2Mit91	D2Mit92		
Chromosome 3 (11)									
	D3Mit200	D3Mit203	D3Mit230	D3Mit28	D3Mit29	D3Mit3	D3Mit305	D3Mit323	D3Mit361
	D3Mit46	D3Mit90							
Chromosome 4 (37)									
	D4Mit116	D4Mit122	D4Mit126	D4Mit134	D4Mit146	D4Mit169	D4Mit18	D4Mit180	D4Mit181
	D4Mit190	D4Mit203	D4Mit219	D4Mit225	D4Mit226	D4Mit227	D4Mit234.2	D4Mit251	D4Mit255
	D4Mit26	D4Mit27	D4Mit272	D4Mit285	D4Mit310	D4Mit33	D4Mit331	D4Mit336	D4Mit348
	D4Mit354	D4Mit357	D4Mit42	D4Mit43	D4Mit45	D4Mit65	D4Mit71	D4Mit81	D4Mit84
	D4Nds3								
Chromosome 5 (22)									
	D5Mit10	D5Mit101	D5Mit108	D5Mit115	D5Mit13	D5Mit134	D5Mit23	D5Mit233	D5Mit239
	D5Mit254	D5Mit26	D5Mit291	D5Mit297	D5Mit314	D5Mit338	D5Mit348	D5Mit371	D5Mit406
	D5Mit425	D5Mit65	D5Mit79	D5Mit93					
Chromosome 6 (4)									
	D6Mit345	D6Mit366	D6Mit8	D6Mit254					
Chromosome 7 (5)									
	D7Mit232	D7Mit259	D7Mit27	D7Mit39	D7Nds5				
Chromosome 8 (3)									
	D8Mit14	D8Mit224	Mt2(D8Mit15)						
Chromosome 9 (3)									
	Cyp1a2(ch#9)		D9Mit2	D9Mit279					
Chromosome 10 (16)									
	D10Mit115	D10Mit134	D10Mit15	D10Mit150	D10Mit186	D10Mit20	D10Mit209	D10Mit214	D10Mit230
	D10Mit261	D10Mit266	D10Mit282	D10Mit297	D10Mit313	D10Mit36	D10Mit61		
Chromosome 11 (3)									
	D11Mit157	D11Mit2	Hoxb(Ch#11)						
Chromosome 12 (4)									
	D12Mit158	D12Mit190	D12Mit231	D12Mit292					
Chromosome 13 (9)									
	D13Mit110	D13Mit186	D13Mit24	D13Mit253	D13Mit26	D13Mit283	D13Mit35	D13Mit48	D13Mit69
Chromosome 14(3)									
	D14Mit2	D14Mit95	D14Nds5						
Chromosome 15(5)									
	D15Mit234	D15Mit29	D15Mit34	D15Mit6	D15Mit90				
Chromosome 16 (7)									
	D16Mit110	D16Mit13	D16Mit211	D16Mit5	D16Mit57	D16Mit88	D16Mit94		
Chromosome 17 (11)									
	D17Mit11	D17Mit119	D17Mit152	D17Mit155	D17Mit176	D17Mit21	D17Mit221	D17Mit266	D17Mit51
	D17Mit52	D17Mit96							
Chromosome 18 (3)									
	D18Mit3	D18Mit40	D18Mit60						
Chromosome 19 (7)									
	D19Mit10	D19Mit10	D19Mit128	D19Mit18	D19Mit8	D19Mit85	D19Mit90		
Chromosome X (25)									
	DXMit119	DXMit121	DXMit143	DXMit149	DXMit154	DXMit156	DXMit16	DXMit189	DXMit197
	DXMit199	DXMit236	DXMit248	DXMit249	DXMit31	DXMit5	DXMit54	DXMit55	DXMit64
	DXMit67	DXMit73	DXMit74	DXMit84	DXMit89	DXMit95	DXMit99		

Fig. 1. A list of markers examined difference between C3H and CBA mouse in a total 256 markers.

parametric statistical analysis for establishing genetic linkage. Contingency tables consisting of affected and non-affected C3H/C3H and C3H/CBA strains were constructed, and chi square (χ^2) tests were performed with one degree of freedom. As recommended by Lander and Kruglyak, $P<0.0034$ ($\chi^2>8.58$) were the thresholds for suggestive linkage (10).

Production of inflammatory cytokines after exposure to CADS. To clarify the inflammatory cytokine response against CADS, we also examined the sequential change of serum cytokines after intraperitoneal injection of CADS. Twenty milligrams of CADS suspended in 0.2 ml of PBS(−) was injected intraperitoneally to C3H/HeN. Sera were obtained from sacrificed mice at each time ($N=5$) for 14 days after injection of CADS and then frozen at −80 C. Serum cytokines, such as interleukins IL-1β, IL-4, IL-6, IL-12, TNF-α, and IFN-γ were measured by using ELISA assay kits: IL-1β, IL-4, IL-6, IL-12, and TNF-α (Genzyme, Mass., U.S.A.), and IFN-γ (Pierce ENDOGEN, Qld, Australia).

Results

Histological Observations of Arteritis

Table 1 shows the incidence of vasculitis in the coronary artery and/or the aortic root in (CBA/JN×C3H/HeN)F1, (C3H/HeN×CBA/JN)F1, and [(CBA/JN×C3H/HeN)×C3H/HeN]N1 was 0%, 16.7%, and 20.7% respectively, while that in C3H/HeN parents was 71.1% (27/38), but in CBA/JN absence (0%, 0/27). Most cases of vasculitis were observed in the aortic root and/or the coronary artery (Fig. 2). All layers of these vessels showed severe inflammation, which is defined as 'productive granulomatous inflammation, but fibrinoid necrosis was rarely determined.' Intima showed various degrees of fibrocellular thickening associated with the lumen of coronary artery became stenotic. In addition to the disruption of internal and external elastic laminas, smooth muscle cells in media deteriorated from severe inflammation. Furthermore, the destruction of the normal structure of the coronary artery in some cases caused aneurismal dilatation. However, neither thrombotic occlusion nor myocardial infarction was observed. Histological differences of arteritis between N1 and C3H/HeN was not elucidated. Arteritis in other visceral organs such as renal artery, testicular artery, and abdominal aorta were rarely detected.

Linkage Analysis with Chromosome Mapping

Two hundred and fifty-six microsatellite markers were tested to segregate loci by original parental strains (Fig. 1). However, most markers were the same sequence length polymorphism between C3H/NeN and CBA/JN. Only 48 markers were selected for the linkage analysis (Table 2). Genome-wide interval mapping analysis between coronary artery and genetic markers for the identification of susceptibility loci was performed by using χ^2 test as described in "Materials and Methods." The markers on the chromosome 1 showed the association even though possibility on other chromosome loci may exist. Two of 11 markers on chromosome 1, *D1Mit171* and *D1Mit245* around 20.2 cM revealed suggestive linkage with P value of 0.0019 (Table 3). The other markers on chromosome 1 did not indicate the association. Based on the suggestive level of *D1Mit171* and *D1Mit245*, this region is thought to influence to the development of coronary arteritis. On the other chromosomes, the marker, *D4Mit285*, showed low probability of 0.017, but was not in the scope to designate an association.

Table 1. Affected rate of coronary arteritis after 9 weeks challenge with CADS

Mice	Affected rate (%)
C3H/HeN	71.1 (27/38)
CBA/JN	0 (0/27)
(C3H male×CBA female) F1	0 (0/9)
(C3H female×CBA male) F1	16.7 (1/6)
(CBA female×C3H male) F1×C3H	20.7 (24/115)

CBA/JN and C3H/HeN (CBA/JN×C3H/HeN) and N1 backcross progeny between F1 and C3H/HeN [(CBA/JN×C3H/HeN)×C3H/HeN] were prepared.

Circulation of Inflammatory Cytokines after Exposure to CADS

Sequential changes of inflammatory cytokines IL-12, IL-1β, TNF-α, IL-6, IFN-γ, and IL-4 in serum for 14 days after intraperitoneal injection of CADS were measured by ELISA assay. Both IL-1β and IL-12 levels in serum increased at 1 hr after injection of CADS, and then decreased gradually, but IL-12 did not decrease like profile of IL-1β (Fig. 3a). After increases of IL-1β and IL-12, levels of TNF-α and IL-6 peaked at 3 hr after the injection, and then restored to baseline by 24 hr (Fig. 3b). Levels of IFN-γ gradually increased over the same period, but no change in IL-4 level was noted (Fig. 3c).

Discussion

Some infectious microorganisms have been implicated in the etiology of KD, though primary causes remain an enigma (6, 11, 16, 22). These candidates of etiology may act as initial trigger to induce arteritis. The spontaneous arteritis model may not be well suited for study-

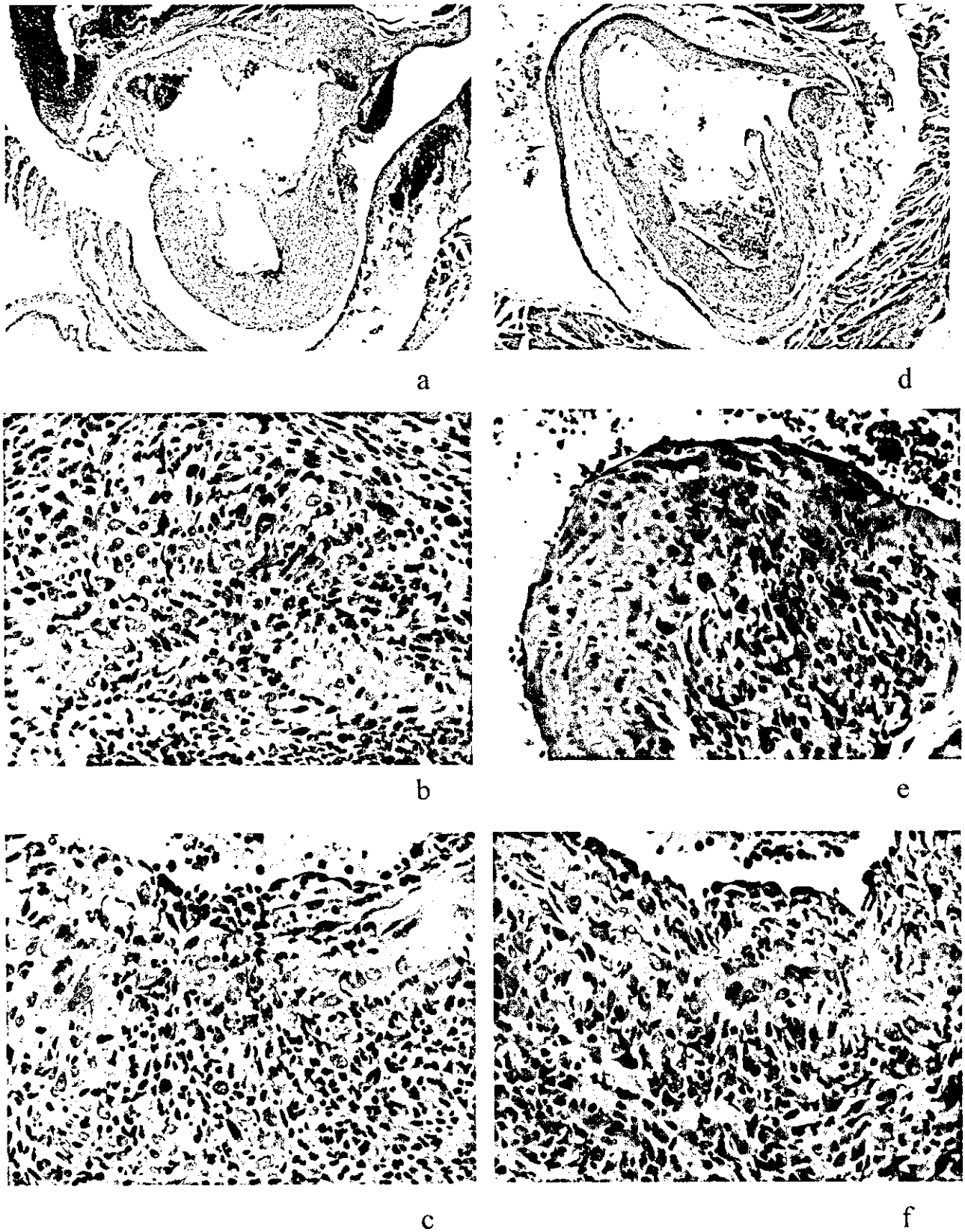

Fig. 2. Histological feature of coronary arteritis in N1 and C3H/HeN. (a) Vasculitis at the coronary artery and aortic root in N1 mouse (HE stain, ×40), (b) coronary arteritis in N1 mouse (HE stain, ×400), (c) aortitis in N1 mouse (HE stain, ×400), (d) coronary arteritis and aortitis in C3H/HeN (HE stain, ×40), (e) coronary arteritis in C3H/HeN (HE stain, ×400), (f) aortitis in C3H/HeN (HE stain, ×400).

Table 2. A list of the 48 markers used for the linkage analysis from 256 candidates for markers

Chromosome	Symbol	Position (cM)	Chromosome	Symbol	Position (cM)
1	D1Mit374	19.0	6	D6Mit345	46.0
1	D1Mit171	20.2	7	D7Mit232	26.8
1	D1Mit245	20.2	8	D8Mit224	17.0
1	D1Mit75	32.1	8	Mt2	45.0
1	D1Mit380	36.9	8	D8Mit14	67.0
1	D1Mit251	38.1	9	D9Mit2	17.0
1	D1Mcg3	38.9	9	Cyp1a2	31.0
1	D1Mcg6	39.9	9	D9Mit279	67.0
1	D1Mit7	41.0	10	D10Mit214	19.0
1	D1Mit200	80.0	11	Hoxb	56.0
1	Tgfbm2	106.3	12	D12Mit231	48.0
2	D2Mit92	41.4	13	D13Mit110	47.0
2	D2Mit206	51.4	14	D14Mit2	5.0
2	D2Mit311	83.1	14	Nfl	28.7
2	D2Mit456	86.3	15	D15Mit6	13.7
2	D2Mit265	105.0	16	D16Mit5	38.0
2	D2Mit200	107.0	17	D17Mit96	54.6
2	D2Mit457	108.0	18	D18Mit60	16.0
3	D3Mit90	4.6	19	D19Mit128	10.9
3	D3Mit200	77.3	19	D19Mit10	47.0
3	D3Mit323	84.9	X	DXMit74	20.0
4	D4Mit272	21.9	X	DXMit16	37.0
4	D4Mit285	71.0	X	DXMit121	67.0
4	D4Mit357	81.5			
5	D5Mit101	81.0			

Table 3. A list of markers that exhibited distribution disequilibrium from the 2×2 χ^2 based on a ratio of affected C3H/C3H:C3H/CBA to non-affected

Chromosome	Distance (cM)	Marker	Affected / Non-affected	χ^2	Probability
1	19.0	D1Mit374	18:6 / 34:45	7.52	0.0061
	20.2	D1Mit171	19:5 / 34:45	9.62	0.0019[a]
	20.2	D1Mit245	19:5 / 34:45	9.62	0.0019[a]
	32.1	D1Mit75	18:6 / 33:46	8.13	0.0044
	38.1	D1Mit251	17:7 / 30:49	8.01	0.0046
	38.9	D1Mcg3	15:9 / 31:48	4.03	0.0447
	39.9	D1Mcg6	15:9 / 31:48	4.03	0.0447
	41.0	D1Mit7	15:9 / 31:48	4.03	0.0447
4	71.0	D4Mit285	7:17 / 45:34	5.69	0.0171

[a] Suggestive linkage.

ing KD, because it requires an initial trigger from some infectious microorganisms to induce arteritis. On the other hand, our model requires injection of CADS to induce arteritis. This model is very useful for the study of the pathogenesis of arteritis in KD for two main reasons: 1) both the histological features and distribution of arteritis are similar to that of KD, and 2) infectious agents are required to induce the development of arteritis. The mechanisms of developing arteritis in patients with KD are still unclear; however, several reports have

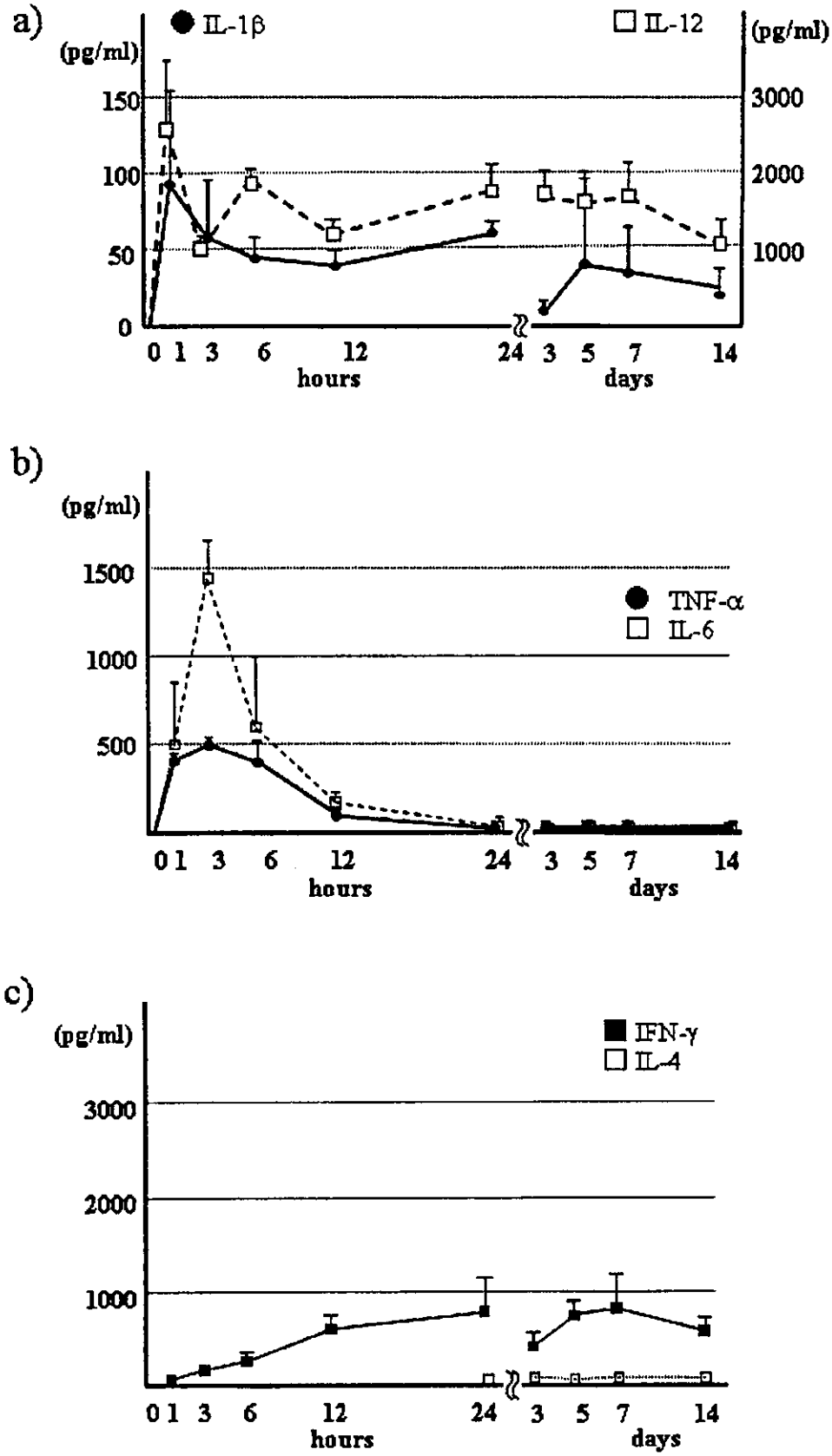

Fig. 3. Time course of serum cytokines after intraperitoneal injection of CADS. (a) Time course of serum IL-1β and IL-12 after injection of CADS, (b) time course of serum TNF-α and IL-6 after injection of CADS, (c) time course of serum IFN-γ and IL-4 after injection of CADS.

discussed the role of inflammatory cytokines in patients with a genetic predisposition to developing coronary arteritis (7, 8). The animal model is considered to be very useful for clarifying the pathogenesis of arteritis in these patients and may allow for the identification of specific treatments for the disease. With the observed differences in the incidence of arteritis in C3H/HeN mice and CBA/JN mice, it can be derived that genetic differences of the mouse strains does influence arteritis. Therefore, it was considered that C3H/HeN may express or attenuate the expression of genes that govern the susceptibility to coronary arteritis.

In the present study, we showed that the loci governing suggestive susceptibility to coronary arteritis were situated on chromosome 1 even though possibility on other chromosome loci may exist. Two of 11 markers on chromosome 1, *D1Mit171* and *D1Mit245* (map position 20.2 cM), appeared to be involved in the susceptibility loci to the development of coronary arteritis. This chromosomal region influences the IL-1 receptors types 1 and 2 (*Il1r1* and *Il1r2*, 19.5 cM). In addition, our results here revealed that IL-1β in sera rapidly increased after intraperitoneal injection of CADS. These findings suggest a ligand-receptor interaction between IL-1β and the IL-1 receptor, which may affect the onset of arteritis. It has been reported that IL-1β regulates vascular damage *in vitro*. Specifically, IL-1β directly injures endothelial cells; however, mechanisms of endothelial cell injury are unclear. Interestingly, an indirect role of IL-1β in the regulation of neutrophil-mediated killing of endothelial cells has been reported (3, 4, 12, 18). Adhesive interaction between activated neutrophils and endothelial cells was facilitated by exposure to IL-1β and superoxide anion, produced by activated neutrophils, and subsequently damaged neighboring endothelial cells (1).

One of the peculiar histological features of arteritis in this model was the severe neutrophilic infiltration observed in the afflicted artery, suggesting an important role of neutrophil activation in the development of arteritis. In addition, it has been reported that the specific antigen to autoantibodies, myleoperoxidase-anti-neutrophil cytoplasmic antibody (MPO-ANCA), targeting its antigen MPO were closely related to the development of coronary arteritis using MPO-deficient mice (17). It is considered that coronary arteritis in this model must be genetically regulated by interactions between neutrophils and endothelial cells modulated by IL-1β. Furthermore, the allelic polymorphism of both *Il1r1* and *Il1r2* and the functional relevance of their polymorphism may be a necessity.

On the other hand, *D4Mit285* (map position 71.0 cM) on chromosome 4 showed negative effect against affectability to coronary arteritis, however this marker showed a probability of 0.017. Several genes related to inflammation are coded around *D4Mit285* on chromosome 4, including TNF receptor superfamily member 1b, 8, and 9 (*Tnfrsf1b*, *Tnfrsf8*, and *Tnfrsf9*) (75.5 cM). The functional relevance of this is seen with the rapid increase of TNF-α following elevation of IL-1β after exposure to CADS. There are also studies that claim IL-1β and TNF-α can induce endothelial cell injury by activated neutrophils (3, 4, 12, 18). Therefore, some of these genes are considered to be protective against the development of coronary arteritis, even in the susceptible C3H/HeN strain. However, the marker *D2Mit265* ($\chi^2=3.61$, $P=0.058$) on chromosome 2, on which IL-1β is located, did not indicate a significant difference. Th-1 cytokines, such as IL-12 and IFN-γ were also produced by exposure of CADS. It was considered that Th-1 type immunity might have an influence on the development of arteritis in this model; however, we have no direct evidence in the present study to determine whether or not the genes of these cytokines affected the coronary arteritis outcome, since the number of microsatellite markers was insufficient to examine these genomic regions.

The difference in the incidence of coronary arteritis between C3H/HeN and CBA/JN may be attributed to differences in the regulation of genes encoding inflammatory cytokines. It may be concluded from the present study that the development of coronary arteritis is multi-factorial and controlled with cumulative effects of these multiple gene loci in this mouse model.

The authors thank Ms. Hitomi Yamada for her technical assistance and, Drs. Kei Takahashi in Toho University Medical School, Akiko Okawara in National Institute of Infectious Diseases and Masato Nose in Ehime University Medical for their helpful discussion in this work. This study was supported in part by Project Research Grants No. 11-26, 12-30, and 13-19 from the Toho University School of Medicine, Ministry of Education, Culture, Sports, Science and Technology for KT and KS, Ministry of Health, Labour and Welfare for KT and KS, Japan Health Science Foundation for KS, and a research fellowship from the Japan Society for the Promotion of Science for ASP. All experiments described in this study were performed in accordance with the current laws of Toho University and National Institute of Infectious Diseases in Japan.

References

1) Alex, B.L., and Peter, A.W. 2000. Regulation of inflammatory vascular damage. J. Pathol. **190**: 343–348.
2) Atobe, T., and Murata, H. 1987. Morphological studies of experimental arteritis—relation with coronary arteritis in Kawasaki disease—. Angiology **27**: 625–633.
3) Borgmann, S., Endisch, G., Hacker, U.T., Song, B.S., and

Fricke, H. 2003. Proinflammatory genotype of interleukin-1 receptor antagonist is associated with ESRD in proteinase 3-ANCA vasculitis patients. Am. J. Kidney Dis. **41**: 933–942.
4) Gonzalez-Gay, M.A., Di Giovine, F.S., Silvestri, T., Amoli, M.M., Garcia-Porrua, C., Thomson, W., Ollier, W.E., and Hajeer, A.H. 2002. Lack of association between IL-1 cluster and TNF-alpha gene polymorphism and giant cell arteritis. Clin. Exp. Rheumatol. **20**: 431.
5) Gu, L., Weinreb, A., Wang, X.P., Zack, D.J., Qiao, J.H., Weisbart, R., and Lusis, A.J. 1998. Genetic determinants of autoimmune disease and coronary vasculitis in the MRL-lpr/lpr mouse model of systemic lupus erythematosus. J. Immunol. **161**: 6999–7006.
6) Hamashima, Y., Tasaka, K., Hoshino, T., Nagata, N., Furukawa, F., Kao, T., and Tanaka, H. 1982. Mite-associated particles in Kawasaki disease. Lancet **2**: 266.
7) Jibiki, T., Terai, M., Shima, M., Ogawa, A., Hamada, H., Kanazawa, M., Yamamoto, S., Oana, S., and Kohno, Y. 2001. Monocyte chemoattractant protein 1 gene regulatory region polymorphism and serum levels of monocyte chemoattractant protein 1 in Japanese patients with Kawasaki disease. Arthritis Rheum. **44**: 2211–2212.
8) Kamizono, S., Yamada, A., Higuchi, T., Kato, H., and Itoh, K. 1999. Analysis of tumor necrosis factor-alpha production and polymorphisms of the tumor necrosis factor-alpha gene in individuals with a history of Kawasaki disease. Pediatr. Int. **41**: 341–345.
9) Kawasaki, T., Kosaki, F., and Okawa, S. 1974. A new infantile acute febrile mucocutaneous syndrome (MCLS) prevailing in Japan. Pediatrics **54**: 271–276.
10) Lander, E., and Kruglyak, L. 1995. Genetic dissection of complex traits: guidelines for interpreting and reporting linkage results. Nat. Genet. **11**: 241–247.
11) Meissner, H.C., and Leung, D.Y. 2000. Superantigens, conventional antigens and the etiology of Kawasaki syndrome. Pediatr. Infect. Dis. **19**: 91–94.
12) Meyrick, B., Christman, B., and Jesmok, G. 1991. Effects of recombinant tumor necrosis factor-alpha on cultured pulmonary artery and lung microvascular endothelial monolayers. Am. J. Pathol. **138**: 93–108.
13) Murata, H. 1979. Experimental *Candida*-induced arteritis in mice, relation to arteritis in the mucocutaneous lymph node syndrome. Microbiol. Immunol. **23**: 825–831.
14) Naoe, S., Atobe, T., and Murata, H. 1983. Experimental coronary arteritis induced by an alkali extract of *Candida albicans* in stool of Kawasaki disease patient. Pediatr. Jpn. **23**: 257–261.
15) Naoe, S., Takahashi, K., Masuda, H., and Tanaka, N. 1991. Kawasaki disease. With particular emphasis on arterial lesions. Acta Pathol. Jpn. **41**: 785–797.
16) Ohkuni, H., Todome, Y., Mizuse, M., Ohtani, N., Suzuki, H., Igarashi, H., Hashimoto, Y., Ezaki, T., Harada, K., and Imada, Y. 1993. Biologically active extracellular products of oral viridans streptococci and the aetiology of Kawasaki disease. J. Med. Microbiol. **39**: 352–362.
17) Okawara, I.A., Oharaseki, T., Takahashi, K., Hashimoto, Y., Aratani, Y., Koyama, H., Maeda, N., Naoe, S., and Suzuki, K. 2001. Contribution of myeloperoxidase to coronary artery vasculitis associated with MPO-ANCA production. Inflammation **25**: 381–387.
18) Schuger, L., Varani, J., Marks, R.M., Kunkel, S.L., Johnson, K.J., and Ward, P.A. 1989. Cytotoxicity of tumor necrosis factor-alpha for human umbilical vein endothelial cells. Lab. Invest. **61**: 62–68.
19) Takahashi, K., Oharaseki, T., and Naoe, S. 2001. Pathological study of postcoronary arteritis in adolescents and young adults: with reference to the relationship between sequelae of Kawasaki disease and atherosclerosis. Pediatr. Cardiol. **22**: 138–142.
20) Takahashi, K., Oharaseki, T., Wakayama, M., Yokouchi, Y., Naoe, S., and Murata, H. 2004. Histopathological features of murine systemic vasculitis caused by *Candida albicans* extract—an animal model of Kawasaki disease. Inflamm. Res. **53**: 72–77.
21) Yamada, A., Miyazaki, T., Lu, L.-M., Ono, M., Ito, R.M., Terada, M., Mori, S., Hata, K., Nozaki, Y., Nakatsuru, S., Nakamura, Y., Onji, M., and Nose, M. 2003. Genetic basis of tissue specificity of vasculitis in MRL/lpr mice. Arthritis Rheum. **48**: 1445–1451.
22) Yoshioka, T., Matsutani, T., Toyosaki, M.T., Suzuki, H., Uemura, S., Suzuki, R., Koike, M., and Hinuma, Y. 2003. Relation of streptococcal pyogenic exotoxin C as a causative superantigen for Kawasaki disease. Pediatr. Res. **53**: 403–410.

Microbiol. Immunol., 48(12), 985–994, 2004

Editor-Communicated Paper

Quantum Dots Targeted to the Assigned Organelle in Living Cells

Akiyoshi Hoshino[1,2,3], Kouki Fujioka[1], Taisuke Oku[1,4], Shun Nakamura[5], Masakazu Suga[1], Yukio Yamaguchi[4], Kazuo Suzuki[3], Masato Yasuhara[2], and Kenji Yamamoto*[,1,2]

[1]Department of Medical Ecology and Informatics, Research Institute, International Medical Center of Japan, Shinjuku-ku, Tokyo 162–8655, Japan, [2]Department of Pharmacokinetics and Pharmacodynamics, Hospital Pharmacy, Tokyo Medical and Dental University, Bunkyo-ku, Tokyo 113–8519, Japan, [3]Department of Bioactive Molecules, National Institute of Infectious Diseases, Shinjuku-ku, Tokyo 162–8640, Japan, [4]Department of Chemical System Engineering, School of Engineering, University of Tokyo, Bunkyo-ku, Tokyo 113–8656, Japan, and [5]Division of Biochemistry and Cellular Biology, National Institute of Neuroscience, Kodaira, Tokyo 187–8502, Japan

Communicated by Dr. Hidechika Okada: Received October 8, 2004. Accepted October 21, 2004

***Abstract*: Fluorescent nanocrystal quantum dots (QDs) have the potential to be applied to bioimaging since QDs emit higher and far longer fluorescence than conventional organic probes. Here we show that QDs conjugated with signal peptide obey the order to transport the assigned organelle in living cells. We designed the supermolecule of luminescent QDs conjugated with nuclear- and mitochondria-targeting ligands. When QDs with nuclear-localizing signal peptides were added to the culture media, we can visualize the movements of the QDs being delivered into the nuclear compartment of the cells with 15 min incubation. In addition, mitochondrial signal peptide can also transport QDs to the mitochondria in living cells. In conclusion, these techniques have the possibility that QDs can reveal the transduction of proteins and peptides into specific subcellular compartments as a powerful tool for studying intracellular analysis *in vitro* and even *in vivo*.**

***Key words*: Quantum dot, Signal peptide, Nanocrystal, Nuclear localizing signal, Mitochondria targeting signal, Bioimaging**

Nanotechnology is the technology of designing, manufacturing, and utilizing the "supermolecule materials" which have the specific function based on their nanometer size. The "supermolecule" said here is a functional unit of two meanings; (1) A supermolecule consists of each molecule that has a certain mutual interaction and relation with one another, (2) A supermolecule shows its specific function as a whole molecule. Ultrafine nanocrystals have been expected to be applied widely in biomedical fields as biomaterials, immunoassay, diagnostics, and even in therapeutics (7, 9, 18, 32, 34, 40, 41). One of them, nanocrystal quantum dots (QDs), is widely used as stable and bright fluorophores that can have high quantum yields, narrow luminescent spectra, high absorbency, high resistance to photobleaching, and can provide excitation of several different emission colors using a single wavelength for excitation (4, 19).

In the field of molecular biology, fluorescent tagging of cells and biomolecules with organic fluorophores such as FITC has been used for a long time for these purposes of tracking biomolecules. But unfortunately, the use of organic fluorophores for living-cell applications is subject to certain limitations, because most of fluorophores photobleach easily (17). These organic fluorophores have their broad emission bands, which limit the number of fluorescent probes that can be simultaneously resolved. In addition, there are a lot of bright fluorophores, such as Hoechst® dyes and a rhodamine 123 derivative (Mitotracker®) (20), used for stain of nuclei and mitochondria, but these fluorophores cannot transport proteins or other molecules to the target

**Address correspondence to* Dr. Kenji Yamamoto, Department of Medical Ecology and Informatics, Research Institute, International Medical Center of Japan, Toyama 1–21–1, Shinjuku-ku, Tokyo 162–8655, Japan. Fax: +81–3–3202–7364. E-mail: backen@ri.imcj.go.jp

Abbreviations: MPA, 3-mercaptopropanoic acid; QD, quantum dot; TOPO, *n*-trioctylphosphine oxide.

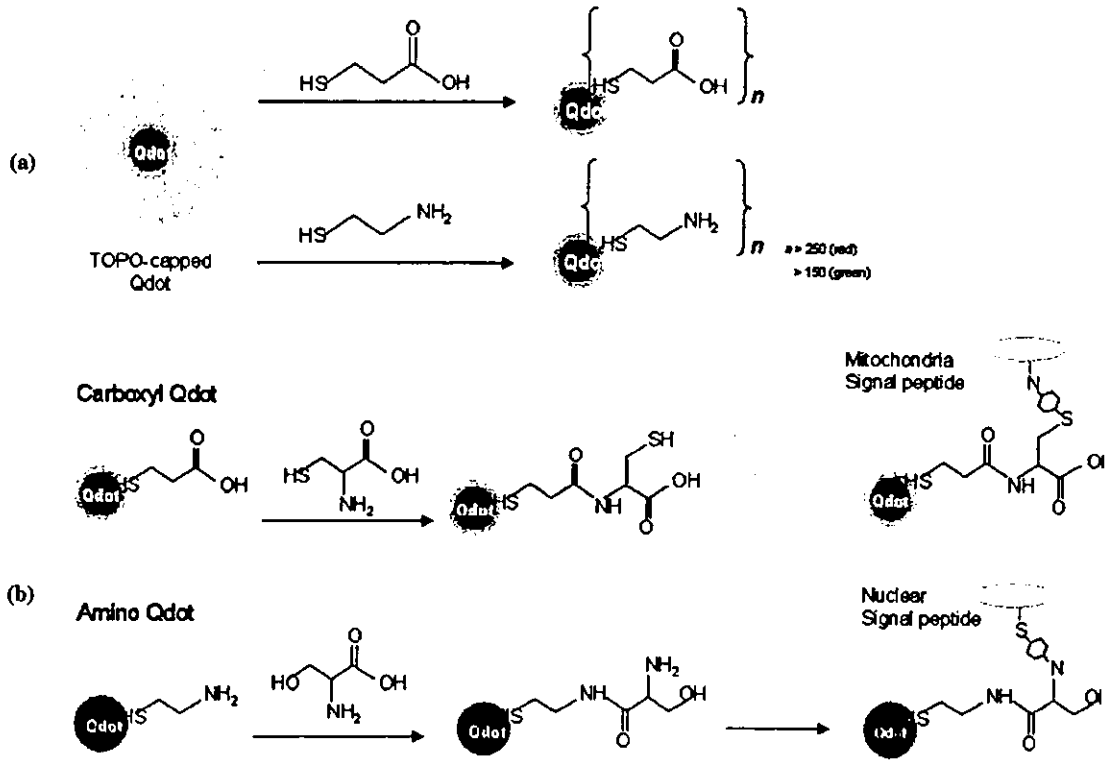

Fig. 1. Schematic illustration of peptide conjugated QDs for organelle targeting and imaging. (a) Chemically synthesized TOPO-capped QDs were replaced by MPA or cysteamine using thiol-exchange reactions. After reaction, QDs were covered with approximately 250 carboxyl or amine groups per particle. (b) A two-step conjugation strategy of QD-oligopeptide probes. MPA-QD (upper lane) or cysteamine-QD (lower lane) was primarily coupled with amine groups of cysteine or serine by using EDC coupling reagents. Then amino acid-coated QDs were secondarily conjugated with target peptides by coupling between *N*-hydroxysuccinimidyl and maleimide groups.

organelle. On the other hand, the signal peptides with organic fluorophore cannot trace the luminescent for long time observation. In contrast, QDs are stabilized over a far longer exposure-time to light and can emit fluorescence of higher luminosity than the conventional organic fluorescence probes (5, 8, 27). Therefore, QDs are suitable for designing the supermolecule that supplemented the biological effects to itself, and applications with QDs are now widely performed as long-time fluorescent markers for efficient collection of fluorescence (3, 17, 22, 24, 35).

Once our synthesized QDs were enfolded into the hydrophobic micelles and completely dissolved in aqueous solution, which promotes several innovations to improve the solubility to apply for biological methods (2, 10, 11, 23). The water-soluble QDs in our previous method have lower stability for low pH or salt-containing buffer (14). There is very little amount of conjugate by using these QDs, since the most of QDs were easily aggregated under the conditions that combine QD with peptides or protein. Therefore, we could only utilize QDs as the high fluorescence cell-tracking markers (14, 33). We previously reported that several novel surface-modified QDs using carboxylic acids, polyalcohols, or amines showed various physicochemical properties (16). In this article, we established a two-step conjugating method as shown in Fig. 1. The QDs of carboxyl groups were primarily coupled with amine groups of cysteine monomer, and QDs of amine groups were with carboxylic groups of serine monomer, respectively. The obtained amino acid-coated QDs, which were stable for the pH changes, were secondarily conjugated with target peptides/proteins by using their sulfhydryl and amine groups.

Some proteins and peptides have been demonstrated to penetrate through the plasma membrane of cells by their protein transduction domains (12, 21, 26, 31). Previous studies defined that protein transduction by nuclear localizing peptides was an efficient method to deliver proteins into the nuclei of cells (25, 37). In this study we tried to label two functional oligopeptides transported to nuclear localizing or mitochondria, and

evaluated whether QD-peptide complex worked as the specific functional supermolecule based on original peptides.

Materials and Methods

Synthesis of hydrophilic QDs. Synthesis of ZnS-coated CdSe nanocrystal QDs (fluorescence wavelength: approximately 642 nm emitted red, and approximately 518 nm emitted green), which were enfolded into the micelle of *n*-trioctylphosphine oxide (TOPO), was previously reported (6, 15). 3-Mercaptopropanoic acid (MPA) and 2-aminoethanethiol (cysteamine hydrochloride) were used to obtain two kinds of hydrophilic QDs (carboxyl- and amino-QDs) by thiol exchange methods. In the case of carboxyl-QD, 50 mg of TOPO-QDs were dissolved into 1 ml tetrahydrofuran (THF) in a 4 ml-volume flasket, and then 250 μl MPA (Sigma-Aldrich, St. Louis, Mo., U.S.A.) were added. Then the mixture was heated at 85 C for 24 hr. In the case of amino-QD, primarily 250 mg cysteamine (Wako Pure Chemicals, Tokyo) was heated at 85 C in a flask (16). After melting, 50 mg/ml TOPO-QDs in THF was dropped to the flask and heated at 85 C for 2 hr. After the reaction, the turbid solution was collected and centrifuged at maximum speed. After it dried up, purified water was added to the residue, and centrifuged at maximum speed to remove the insoluble residue. The supernatant fraction containing soluble QDs was collected. After purified by Sephadex G-25 column (Amersham Biosciences, Piscataway, N.J., U.S.A.), QDs were concentrated and powderized by vacuum distillation. QDs were reconstituted in purified water before use.

Preparation of peptide-conjugated QDs. Amino acid sequences of three well-known functional oligopeptides described below were chemically synthesized; nuclear localizing peptide ($R_{11}KC$, sequenced NH_2-RRRRRRRRRRRKC-COOH) (25), mitochondria targeting signal sequence of cytochrome-*c* oxidase VIII subunit (Mito-8, sequenced NH_2-MSVLTPLLLRGLTGSARRLPVPRAKIHWLC-COOH) (13) or control mitochondrial peptide (START, sequenced NH_2-STARTSTARTSTARTSC-COOH) (1). The peptides were conjugated to QDs by a two-step reaction. Initially, 100 μM QD solution was mixed with equal volume of 100 mM cysteine solution in coexistent with 100 mM EDC coupling reagents (Pierce Biotechnology, Rockford, Ill., U.S.A.) and continuously mixed at 4 C for 1 hr. After removed of free-amino acid by Nap-5 column (Amersham Biosciences), about 10-fold mol of target peptides were secondarily conjugated with QD by using sulfo-SMCC coupling reagents (Pierce Biotech) and sonicated for 2 hr at 4 C. Products were purified using ultra-filtration membrane (NMWL 10000, Centriprep® Millipore). Finally, purified QD-peptide conjugates were filtrated with 0.1-μm membrane filters (Millipore) before use. To analyze the protein content of QD-conjugated peptides, conjugated QDs was plated to 96-well microplate and RC-DC Protein Assay reagent (Bio-Rad, Hercules, Calif., U.S.A.) was added. Six hundred fifty nanometer absorbance was measured by microplate reader (Bio-Rad). MPA-coated QD without coupling with any peptides was used as negative control.

Assessment of QD-uptake by cells. Vero cells were cultured in DMEM/F12 supplemented with 5% heat-inactivated fetal bovine serum at 37 C. To avoid the non-specific binding of QDs on the glass, 10 mm glass-based culture dish (Matsunami Glass Industries, Japan) was pre-coated with poly-L-lysine (Peptide Institute Co., Ltd., Osaka, Japan). The cells were plated at a volume of 1×10^5 cells/well on a glass-based dish. Then cells were stimulated with the indicated concentration of QD-peptides. After incubation, the cells were washed with PBS 5 times to remove the non-specific binding QDs, and the cells were fixed, and embedded in the glycerol containing 0.1% sodium azide. In the case of co-localization assay, cells were observed with a confocal microscopy MRC-1024 (Bio-Rad). Time course of $R_{11}KC$-coated QDs was examined on the fluorescence microscopy system equipped with a CO_2 incubator (IM-310 cell-culture microscope system, Olympus, Japan). Images were acquired with a digital camera D1X (Nikon) under fluorescent microscopy IX-81 (Olympus) using WIR mirror unit to adjust excitation wavelength over 610 nm.

Results and Discussion

Some oligopeptides have been demonstrated to penetrate across the cellular membrane by their protein transduction domains and specifically located to their designated organelle (12, 21, 26, 31). Previous studies showed that the protein transduction by nuclear localizing signal oligopeptide was an efficient method of delivering proteins into the nuclei of cells (37). To establish the supermolecule design that supplemented the biological effects to nanocrystal, we conjugated two kinds of functional NLS and MTS oligopeptides, which were transported to nuclear or mitochondria (13, 25). Then we evaluated that QD-peptide complex worked as the specific supermolecule those functions were based on their original peptides.

For the achievements of assemble QD-supermolecule, we established a two-step conjugating method as shown in Fig. 1. Briefly, QDs were coupled with amino

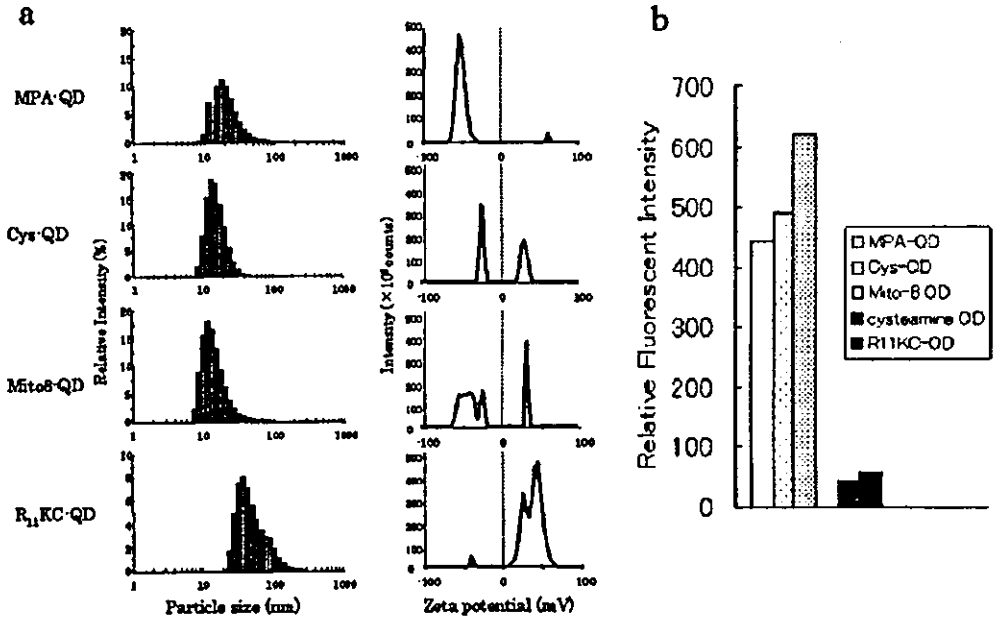

Fig. 2. Physicochemical properties of oligopeptide-conjugated QDs. (a) Particle size distribution of various QDs in aqueous solution (left) was measured by dynamic light scattering methods. Values are the mean±standard deviation of the data measured 12 times, respectively. Surface ζ-potential of QDs (right) was measured by electrophoresis. The line shows the electrophoretic mobility of these QDs in the stationary layers of 30 assays. Data shows the average of 30 assays. (b) Relative fluorescence intensity of QDs solution (10 μM) were measured by fluorospectrometer. QDs were excited by 365 nm wavelength (UV-A) and luminescence intensity of peak emission wavelength (519 nm) was detected.

acid at the first step, and secondarily coupled with the target oligopeptide. We prepare two kinds of QD whose surfaces were covered with carboxyl and sulfhydryl, and with NH_2 and hydroxyl groups, respectively. MPA-QDs were primarily coupled with amine groups of cysteine by using EDC coupling reagents (cys-QD). In the case of amine-QDs, they were also coupled with carboxylic groups of serine (ser-QD). The surface of the obtained QD was covered with approximately 450 amino acids per particle (data not shown). Both of the newly obtained amino acid-coated QDs, which were stable for changes of pH, were secondarily conjugated with target peptides by coupling with their sulfhydryl and amine groups by sulfo-SMCC reagents. In this study, we conjugated two kinds of signaling peptide; nuclear localizing signal (NLS) oligopeptide $R_{11}KC$ (25), and mitochondria targeting signal (MTS) oligopeptide Mito-8 (13). Mito-8 peptides were coupled with cys-QDs, and basic $R_{11}KC$-peptides were with ser-QDs, respectively. The number of peptide with QDs were calculated based on RC-DC protein assay, indicating that QD-$R_{11}KC$ and QD-Mito-8 were covered with 48 and 62 peptides per particle, respectively (data not shown). To assess the change of physicochemical properties of QDs after conjugated with oligopeptides, the particle size and surface potential of peptide-conjugated QDs were observed by a dynamic light scattering method. This surface potential of QDs was drastically changed after conjugated with peptides (Fig. 2a). In this labeling method, the average of the observed particle size distribution tends to increase, because it is hardly avoidable to control the excess polymerization. Previously, we tried to target signal peptides directly to MPA-QDs, resulted in aggregation, especially in the case of amine-rich oligopeptides because of salt-formation between carboxylic groups of QD and amine groups of target peptides (16). This novel two-step method enables to QDs labeled even in amine-rich basic oligopeptides such as $R_{11}KC$. Our previous study demonstrated that the fluorescence intensity of QD was also dramatically changed by the surface-covered molecules of QD particle (16, 22). We previously tried to cover QDs directly with cysteine monomer, which resulted in losing luminescence during the labeling process, because of electron leakage through the surface NH_2 group (16). Therefore, we assessed whether the fluorescent intensity of QDs changed or diminished during the peptide coupling process. After the first reaction step, slight change of luminescent intensity was observed. But the fluores-

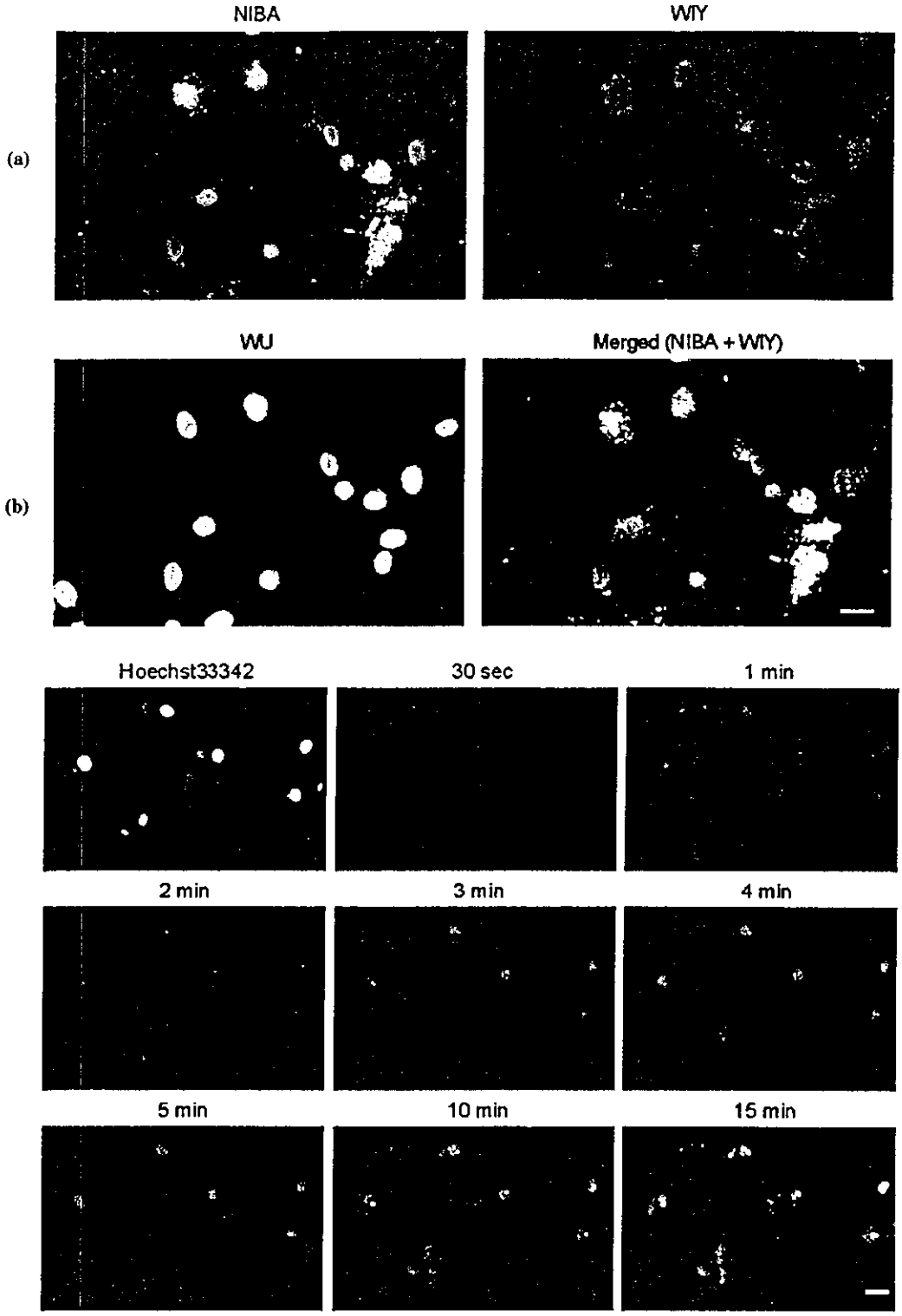

Fig. 3. Localization of R_{11}KC-conjugated QDs to nucleus. (a) Cells were pre-stained with Hoechst®33342, and stimulated with FITC-labeled QD-conjugated R_{11}KC peptide (1 μM final) for 3 hr at 37 C with 5% CO_2 condition. (b) Cells were pre-stained with Hoechst®33342, and stimulated with QD-R^{11}KC (1 μM final) for the indicated time at 37 C under 5% CO_2 condition with a culture fluorescence microscope (IM-310 system, Olympus). Images were taken using D1X digital camera (Nikon) equipped with IM-310 system at the indicated time by a 3 sec exposure. Bars indicated 10 μm.